

### 4.3 Diagrammatic rules in the energy domain

Now that the mapping and the back-mapping between diagrams and analytical expression in the time domain has been fully clarified, we make the further step of mapping the diagrams directly to the energy domain. This last step is particularly useful since the Laplace transform of the time domain kernel is the one determining the stationary density matrix. Before giving the general rules we proceed, though, with the derivation of the analytical expression of some of the rates for a specific system.

#### 4.3.1 2<sup>nd</sup> and 4<sup>th</sup> order kernels for the AIM

The Anderson Impurity Model is defined by the Hamiltonian:

$$\hat{H}_{\text{sys}} = \sum_{\sigma \uparrow, \downarrow} \epsilon_{\sigma} \hat{n}_{\sigma} + U \hat{n}_{\uparrow} \hat{n}_{\downarrow} \quad (4.50)$$

where  $\hat{n}_{\sigma} = d_{\sigma}^{\dagger} d_{\sigma}$  counts the number of electrons with spin  $\sigma$  on  $d$  single orbital. The eigenstates and eigenenergies of (4.50) are

Eigenstate	Eigenenergy
$ 0\rangle$	0
$ 1\uparrow\rangle$	$\epsilon_{\uparrow}$
$ 1\downarrow\rangle$	$\epsilon_{\downarrow}$
$ 12\rangle$	$\epsilon_{\uparrow} + \epsilon_{\downarrow} + U = E_2$

As an example we will calculate  $(K^{(2)})_{22}^{22}$  and  $(K^{(4)})_{22}^{22}$  according to (4.45) and (4.46)


Let us start with the 2<sup>nd</sup> order:

$$(K^{(2)})_{22}^{22} = \lim_{\lambda \rightarrow 0} \int_0^{\infty} dt' e^{-\lambda t'} \langle 21 | K^{(2)}(t, t-t') [12 \chi 21] | 2 \rangle \quad (4.51)$$

where the exponentials in (4.45) disappear due to the coincidence of initial and final states. Diagrammatically

$$(K^{(2)})_{22}^{22} = \sum_{\sigma} \left( \begin{array}{c} |2\rangle \xleftarrow{\sigma} \text{---} \text{---} \text{---} |2\rangle \\ \text{---} \text{---} \text{---} \xrightarrow{\sigma} \langle 21| \end{array} + \begin{array}{c} |2\rangle \xleftarrow{\sigma} \text{---} \text{---} \text{---} |2\rangle \\ \text{---} \text{---} \text{---} \xrightarrow{\sigma} \langle 21| \end{array} \right)$$

Notice that, of the 8 diagrams composing the time evolution kernel  $K^{(2)}(t, \tau)$  only 2 survive due to the secularity of the initial and final states.

The selection can be summarized: i) Each contour must contain an in-going and an out-going vertex  $\rightarrow$   is excluded. ii) The direction of the fermionic line is chosen such that ALONG the contour direction the out-going transition precedes the in-going one. Notice: on the lower contour the preparation is backwards in time! The contour and not the time ordering decides which diagrams should be kept into account.

The two graphs are one the h.c. (more properly the complex conjugate) of each other.

$$\begin{aligned} (K^{(2)})_{22}^{22} &= - \lim_{\lambda \rightarrow 0} \sum_{\sigma} \int_0^{\infty} dt' e^{-\lambda t'} \langle \hat{C}_{3,\sigma}^- \hat{C}_{0,\sigma}^+ \rangle \langle 21 | \hat{D}_{3,\sigma}^+ \hat{D}_{0,\sigma}^- | 2 \rangle \langle 21 | 2 \rangle + \text{h.c.} \\ & \quad \mathbb{1} = \sum_a |a\rangle \langle a| \\ &= - \sum_{\sigma} \lim_{\lambda \rightarrow 0} \int_0^{\infty} dt' e^{-\lambda t'} \langle \hat{C}_{3,\sigma}^- \hat{C}_{0,\sigma}^+ \rangle \langle 21 | \hat{D}_{3,\sigma}^+ | \sigma \rangle \langle \sigma | \hat{D}_{0,\sigma}^- | 2 \rangle \langle 21 | 2 \rangle + \text{h.c.} \end{aligned}$$

$$\begin{aligned} (4.47) &= - \frac{1}{\hbar^2} \sum_{\sigma} \lim_{\lambda \rightarrow 0} \int_0^{\infty} dt' e^{-\lambda t'} \sum_{\alpha \vec{k}} f_{\alpha}^-(\omega_{\vec{k}}) e^{-i \omega_{\vec{k}} t' / \hbar} \\ & \quad \cdot \langle 21 | t_{\alpha \vec{k} \sigma}^* t_{\alpha \vec{k} \sigma}^* e^{i \epsilon_2 t' / \hbar} d_{\sigma}^+ | \sigma \rangle \langle \sigma | e^{-i \epsilon_0 t' / \hbar} e^{i \epsilon_1 (t-t') / \hbar} d_{\sigma} e^{-i \epsilon_2 (t-t') / \hbar} | 2 \rangle \\ & \quad + \text{h.c.} = \end{aligned}$$

$$(4.49) \quad -\frac{1}{\hbar^2} \sum_{\alpha} \lim_{\lambda \rightarrow 0} \int d\omega f_{\alpha}^{-}(\omega) \int_0^{\infty} dt' e^{-\lambda t'} e^{-\frac{i}{\hbar}(\omega + \bar{E}_{\bar{\alpha}} - E_2)t'} T_{\alpha\bar{\alpha}}^{+}(2, \bar{\alpha}) \bar{T}_{\alpha\bar{\alpha}}^{-}(\bar{\alpha}, 2) + h.c.$$

$$= -\frac{1}{\hbar^2} \frac{1}{i\hbar} \lim_{\tilde{\lambda} \rightarrow 0} \sum_{\alpha} \int d\omega f_{\alpha}^{-}(\omega) \frac{1}{\omega + \bar{E}_{\bar{\alpha}} - E_2 - i\tilde{\lambda}} |T_{\alpha\bar{\alpha}}^{+}(2, \bar{\alpha})|^2 + h.c.$$

( $\tilde{\lambda} = \hbar\lambda$ )

$$= -\frac{i}{\hbar} \sum_{\alpha} |T_{\alpha\bar{\alpha}}^{+}(2, \bar{\alpha})|^2 \lim_{\lambda \rightarrow 0} \int d\omega \frac{f_{\alpha}^{-}(\omega)}{-\omega + E_2 - \bar{E}_{\bar{\alpha}} + i\lambda} + h.c.$$

$$= -\frac{i}{\hbar} \sum_{\alpha} |T_{\alpha\bar{\alpha}}^{+}(2, \bar{\alpha})|^2 \left\{ \operatorname{Re} \lim_{\lambda \rightarrow 0} \int d\omega \frac{f_{\alpha}^{-}(\omega)}{-\omega + E_2 - \bar{E}_{\bar{\alpha}} + i\lambda} + i \operatorname{Im} \lim_{\lambda \rightarrow 0} \int d\omega \frac{f_{\alpha}^{-}(\omega)}{-\omega + E_2 - \bar{E}_{\bar{\alpha}} + i\lambda} \right\}$$

+ h.c.

Here we make use of a formula which can be proven using residual calculation

$$\textcircled{\text{I}} \quad \lim_{W \rightarrow \infty} \lim_{\eta \rightarrow 0} \operatorname{Re} \int dx \frac{f^{\dagger}(x)}{d(x - \beta, \mu) + i\eta} \frac{W^2}{x^2 + W^2} = d^{\dagger} \left( \operatorname{Re} \psi^{(0)} \left( \frac{1}{2} + \frac{i\beta\mu}{2\pi} \right) - c \right) \quad (4.52)$$

$d, p = \pm$ , where  $\psi^{(0)}(z)$  is the digamma function

$$\psi^{(0)}(z) = -\sum_{n=0}^{\infty} \frac{1}{n+z} + \sum_{n=1}^{\infty} \log \left( 1 + \frac{1}{n} \right) \quad (4.52b)$$

and  $c = \psi^{(0)} \left( \frac{1}{2} + \frac{iW}{2\pi} \right) \quad (4.52c)$

$$\textcircled{\text{II}} \quad \lim_{\eta \rightarrow 0} \operatorname{Im} \int dx \frac{f^{\dagger}(x)}{d(x - \beta, \mu) + i\eta} = -\pi f^{\dagger}(\beta, \mu) \quad (4.53)$$

A detailed proof of (4.52) and (4.53) can be found for example in the Ph.D thesis of Sonja Koller.

We thus define for following purposes

$$\begin{aligned}
 Y_{\pm}^{\text{P}}(\mu) &= Y_{\pm}^{\text{pd}}(\mu) := -\frac{i}{\hbar} \lim_{\eta \rightarrow 0} \int dx \frac{f^{\text{P}}(x)}{d(x - \beta\mu) + i\eta} \\
 &= -\frac{i}{\hbar} \lim_{\eta \rightarrow 0} \lim_{W \rightarrow \infty} \int dx \frac{f^{\text{P}}(x)}{d(x - \beta\mu) + i\eta} \frac{W^2}{x^2 + W^2} \\
 &= -\frac{\pi}{\hbar} f^{\text{pd}}(\beta\mu) - i^{\text{pd}} \left( \text{Re } \Psi^{(0)}\left(\frac{1}{2} + \frac{i\beta\mu}{2\pi} - c\right) \right) \quad (4.54)
 \end{aligned}$$

$$\Rightarrow \left( K^{(2)} \right)_{22}^{22} = \sum_{\alpha \in \sigma} \left| T_{\alpha \bar{\sigma}}^+(2, \bar{\sigma}) \right|^2 Y_{+}^+(E_{\bar{\sigma}} - E_2) + \text{h.c.} \quad (4.55)$$

Notice that the Lorentzian  $\frac{W^2}{x^2 + W^2}$  set an energy cut off that makes  $Y_{\pm}^+(\Delta)$  finite  $\forall W$ .  $Y_{\pm}^+(\mu)$  diverges in the limit  $W \rightarrow \infty$  but this is not the case for  $\left( K^{(2)} \right)_{22}^{22}$  which is always finite. The final result is known

$$\boxed{\left( K^{(2)} \right)_{22}^{22} = -\frac{2\pi}{\hbar} \sum_{\alpha \in \sigma} \mathcal{D}_{\alpha} f^{-}(E_2 - E_{\bar{\sigma}} - \mu_{\alpha})} \quad (4.56)$$

since from the derivation one sees that  $\mu = -E_2 + E_{\bar{\sigma}} + \mu_{\alpha}$ , and  $f_{(-x)}^{\text{P}} = f_{x}^{\text{P}}$ . The full calculation of the  $Y_{\pm}^{\text{P}}(\mu)$  function becomes important for example in presence of degenerate many-body states. These are though absent in the AIM. The simplest model presenting them is the triple dot molecule (see Sheet 12).

Now we want to address the 4<sup>th</sup> order contributions to the same element of the time-evolution kernel

$$(K^{(4)})_{22}^{22} = \lim_{\lambda \rightarrow 0} \int_0^\infty d\tau' e^{-\lambda\tau'} \int_0^{\tau'} d\tau_1' \int_0^{\tau_1'} d\tau_2' \langle 2 | K^{(4)}(t, t-\tau_2', t-\tau_1', t-\tau') | 2 \rangle [12 \times 21] | 2 \rangle$$

$$= \sum_{\sigma} \left[ \begin{array}{c} |2\rangle \leftarrow \begin{array}{c} \sigma \quad \sigma \quad \sigma \quad \sigma \\ \curvearrowright \end{array} |2\rangle \\ \langle 2 | \longrightarrow \langle 2 | \end{array} \right] + \begin{array}{c} |2\rangle \leftarrow \begin{array}{c} \bar{\sigma} \quad \bar{\sigma} \quad \bar{\sigma} \quad \bar{\sigma} \\ \curvearrowright \end{array} |2\rangle \\ \langle 2 | \longrightarrow \langle 2 | \end{array} \quad (4.57)$$

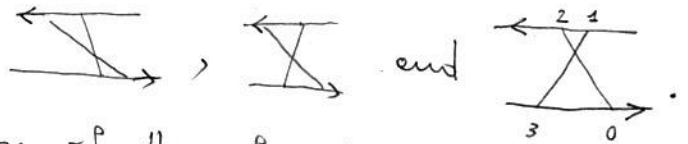
$$+ \sum_{\sigma'} \left( \begin{array}{c} |2\rangle \leftarrow \begin{array}{c} \sigma \\ \curvearrowright \end{array} |2\rangle \\ \langle 2 | \longrightarrow \begin{array}{c} \sigma' \quad \sigma' \\ \curvearrowright \end{array} \langle 2 | \end{array} + \begin{array}{c} |2\rangle \leftarrow \begin{array}{c} 3\sigma \quad 1\sigma \\ \curvearrowright \end{array} |2\rangle \\ \langle 2 | \longrightarrow \begin{array}{c} 2\sigma' \quad 0\sigma' \\ \curvearrowright \end{array} \langle 2 | \end{array} \right)$$

$$+ \left[ \begin{array}{c} |2\rangle \leftarrow \begin{array}{c} \bar{\sigma} \quad \bar{\sigma} \quad \bar{\sigma} \quad \bar{\sigma} \\ \curvearrowright \end{array} |2\rangle \\ \langle 2 | \longrightarrow \langle 2 | \end{array} + \begin{array}{c} |2\rangle \leftarrow \begin{array}{c} \sigma \quad \sigma \\ \diagdown \quad \diagup \\ \sigma \quad \sigma \end{array} |2\rangle \\ \langle 2 | \longrightarrow \begin{array}{c} \sigma \quad \sigma \\ \diagup \quad \diagdown \\ \sigma \quad \sigma \end{array} \langle 2 | \end{array} + \text{h.c.} \right]$$

Now, the restriction rules for extracting the 12 (24) diagrams listed above without (with) the hermitian conjugate contribution, are

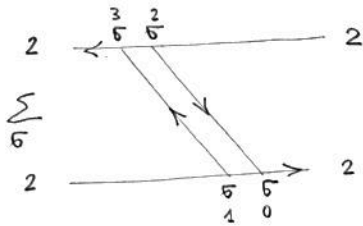
- i \* each contour should have an even number of vertices paired in in and out ones.
- ii \* the first vertex along the orientation must be an out-going one.
- iii \* if the second vertex is out-going (in-going) it must be of opposite (equal) spin with respect to the first one

Rule i) exclude half of 4<sup>th</sup> order diagrams. Rule ii) exclude the three classes of crossed diagrams



Eventually, rule iii) fixes the orientation of the fermionic lines of the residual  $s$  clones and leaves "only" 24 diagrams available.

Exemplarily we calculate the best contribution:



$$= \lim_{\lambda \rightarrow 0} \sum_{\sigma} \int_0^{\infty} d\tau' e^{-\lambda\tau'} \int_0^{\tau'} d\tau_1' \int_0^{\tau_1'} d\tau_2' \langle \hat{C}_{1,\sigma}^+ C_{3,\sigma}^- \rangle \langle \hat{C}_{0,3}^- \hat{C}_{2,\sigma}^+ \rangle$$

$$\langle 2 | \hat{\Delta}_{3,\sigma}^+ | \bar{\sigma} \rangle \langle \bar{\sigma} | \hat{\Delta}_{2,\sigma}^- | 2 \rangle \langle 2 | \hat{\Delta}_{0,\sigma}^+ | \bar{\sigma} \rangle \langle \bar{\sigma} | \hat{\Delta}_{4,\sigma}^- | 2 \rangle$$

$$= \frac{1}{\hbar^4} \lim_{\eta \rightarrow 0} \sum_{\alpha\alpha'\sigma} \int_0^{\infty} d\tau_2' \int_{\tau_2'}^{\infty} d\tau_1' \int_{\tau_1'}^{\infty} d\tau' \int d\omega \int d\omega' f_{\alpha}^+(\omega) f_{\alpha'}^-(\omega')$$

$$e^{i\frac{1}{\hbar}(-\omega + \bar{E}_2 - \bar{E}_{\bar{\sigma}})\tau_1'} e^{i\frac{1}{\hbar}(-\omega' + \bar{E}_2 - \bar{E}_{\bar{\sigma}})\tau_2'} e^{i\frac{1}{\hbar}(\omega' - \bar{E}_2 + \bar{E}_{\bar{\sigma}} + i\eta)\tau'}$$

$$T_{\alpha\bar{\sigma}}^+(2, \bar{\sigma}) T_{\alpha'\bar{\sigma}}^-(\bar{\sigma}, 2) T_{\alpha'\bar{\sigma}}^+(2, \bar{\sigma}) T_{\alpha\bar{\sigma}}^-(\bar{\sigma}, 2)$$

$$= -\frac{i}{\hbar} \lim_{\eta \rightarrow 0} \sum_{\alpha\alpha'\sigma} \int d\omega \int d\omega' f_{\alpha}^+(\omega) f_{\alpha'}^-(\omega') |T_{\alpha\bar{\sigma}}^+(2, \bar{\sigma})|^2 |T_{\alpha'\bar{\sigma}}^-(2, \bar{\sigma})|^2$$

$$\frac{1}{-\omega + \omega' + i\eta} \frac{1}{-\omega + \bar{E}_2 - \bar{E}_{\bar{\sigma}} + i\eta} \frac{1}{\omega' - \bar{E}_2 + \bar{E}_{\bar{\sigma}} + i\eta} \quad (4.58)$$

where for the evaluation of the time ordered integrations, in the last step, the variable transformation  $\tilde{\tau}_2 = \tau_1' - \tau_2'$ ,  $\tilde{\tau} = \tau' - \tau_2'$  which decouple the three time integrations, were applied.



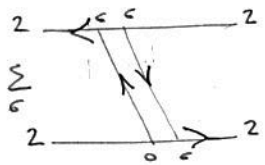
Note: To evaluate the frequency integrals, we notice that the structure is of the form

$$-\frac{i}{\hbar} \int d\omega \int d\omega' f_{\alpha}^{\dagger}(\omega) f_{\alpha'}^{\dagger}(\omega') \frac{1}{\Delta_0} \frac{1}{\Delta_0 + \Delta_1} \frac{1}{\Delta_0 + \Delta_1 + \Delta_2} \quad (4.59)$$

where  $\frac{i}{\hbar} \Delta_{0/1/2}$  where the arguments of the exponentials containing  $\tau, \tau_1, \tau_2$  respectively.

Working with dimensionless coordinates:  $x = \beta\omega$  and remembering that

$$f_{\alpha}^{\dagger}(\omega) = f(\beta(\omega - \mu_{\alpha})) \text{ one obtains}$$



$$= \sum_{\alpha\alpha'} |T_{\alpha\bar{\sigma}}^{\dagger}(z, \bar{\sigma})|^2 |T_{\alpha'\bar{\sigma}}^{\dagger}(z, \bar{\sigma})|^2 \left(-\frac{i}{\hbar} \beta\right) \lim_{\eta \rightarrow 0}$$

$$\int dx \int dx' \frac{f^{\dagger}(x) f^{\dagger}(x')}{x' + \beta\mu_{\alpha'} - \beta(E_2 - E_{\bar{\sigma}}) + i\eta} \frac{1}{-x - \beta\mu_{\alpha} + x' + \beta\mu_{\alpha'}} \frac{1}{-x - \beta\mu_{\alpha} + \beta(E_2 - E_{\bar{\sigma}}) + i\eta}$$

$$x = \beta\omega - \beta\mu_{\alpha}$$

$$x' = \beta\omega' - \beta\mu_{\alpha'}$$

Eventually, this result can be made more compact with the introduction of the function  ${}^{\pm}X_{-}^{\pm}$

$$\sum_{\bar{\sigma}} \int_{\bar{\sigma}}^{\bar{\sigma}} = \sum_{\alpha\alpha'} |T_{\alpha\bar{\sigma}}^{\dagger}(z, \bar{\sigma})|^2 |T_{\alpha'\bar{\sigma}}^{\dagger}(z, \bar{\sigma})|^2 {}^{\pm}X_{-}^{\pm}(\bar{E}_{2\bar{\sigma}} - \mu_{\alpha}, \bar{E}_{2\bar{\sigma}} - \mu_{\alpha'}, \mu_{\alpha} - \mu_{\alpha'}) \quad (4.60)$$

where  $\bar{E}_{2\bar{\sigma}} := E_2 - E_{\bar{\sigma}}$  and the function  ${}^{\pm}X_{-}^{\pm}(\cdot, \cdot, \cdot)$  enters into a more general scheme of fourth order integrals that I present in the next page.

Note: Structure of the fourth-order integrals

To evaluate the fourth order kernel we introduce two types of double integrals:  $\pm X_{dd'}^{pp'}$  and  $\pm \Delta_{dd'}^{pp'}$ , where  $p, p', d, d' \in \{+, -\}$

$$\pm X_{dd'}^{pp'}(\mu, \mu', \Delta) = \frac{\beta}{i\hbar} \lim_{\eta \rightarrow 0} \int dx \int dx' f^{\pm}(x) f^{\pm'}(x')$$

$$\frac{1}{d(x - \beta\mu) + i\eta} \quad \frac{1}{dx + d'x' - \beta\Delta + i\eta} \quad \frac{1}{d(\pm x' - \beta\mu') + i\eta} \quad (4.61)$$

and

$$\pm \Delta_{dd'}^{pp'}(\mu, \mu', \Delta) = \frac{\beta}{i\hbar} \lim_{\eta \rightarrow 0} \int dx \int dx' f^{\pm}(x) f^{\pm'}(x')$$

$$\frac{1}{d(x - \beta\mu) + i\eta} \quad \frac{1}{dx + d'x' - \beta\Delta + i\eta} \quad \frac{1}{d(\pm x - \beta\mu') + i\eta} \quad (4.62)$$

In general these are complicated functions involving products of Fermi/Bose functions with Gamma function's derivatives: the poly gamma functions.

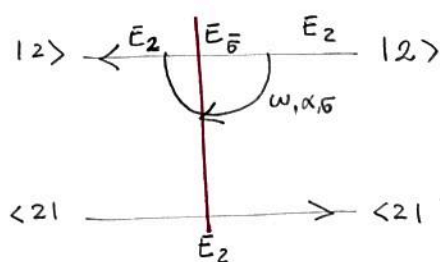


### 4.3.2 Back mapping in energy domain

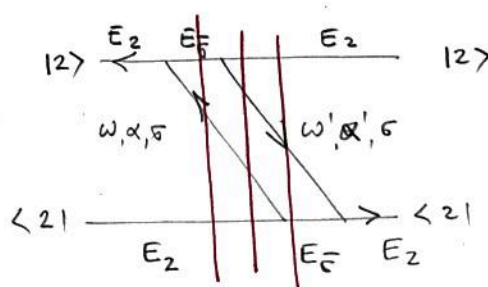
For a given  $2n$ -th order diagram as obtained in the time domain one can write a set of simple rules which allow to obtain at once the multiple energy integral associated to the Laplace transform of the kernel.

- [1] To each of the fermion lines, assign an energy  $\omega_i$ , as well as the lead and spin indices  $\alpha_i, \sigma_i$  respectively ( $1 \leq i \leq n$ ).  
To each section on the contours, assign the energy of the corresponding state

2<sup>nd</sup> order



4<sup>th</sup> order



- [2] Between two consecutive times  $\tau_j$  and  $\tau_{j+1}$  perform a vertical cut. You will obtain  $2n-2$  cuts. From each cut obtain a denominator  $A_j$ : for each intersection of the cut with a fermion line or a contour, one adds up with a specific sign the energy assigned to the fermion line, respectively to the contour at the intersection. Thereby, the sign is determined by the directions of the fermion line, respectively the contour: If they hit the cut from the right, their energy has to be counted negative, if they come from the left, the sign is positive.

$$2^{\text{nd}} \text{ order} \Rightarrow A_0 = E_2 - \omega - \bar{E}_2$$

$$4^{\text{th}} \text{ order} \Rightarrow \begin{aligned} A_0 &= \bar{E}_2 + \omega' - \bar{E}_2 \\ A_1 &= E_2 - \omega + \omega' - \bar{E}_2 \\ A_2 &= E_2 - \omega + \bar{E}_2 \end{aligned}$$

3 For each fermion line, determine a sign  $p_i$  which tells whether it belongs to an in-tunnelling ( $p_i = +$ ) or an out-tunnelling process ( $p_i = -$ ): If the connected vertices lie on the same contour, for a forward pointing line it is  $p_i = -$ ,  $p_i = +$  for a backward one. If the vertices lie on different contours it is vice versa.

$$2^{\text{nd}} \text{ order} \quad p = -$$

$$4^{\text{th}} \text{ order} \quad p_1 = + \quad p' = -$$

4 Determine  $q$ , which is the number of vertices on the lower contour plus the number of crossings of fermion lines

$$2^{\text{nd}} \quad q = 0$$

$$4^{\text{th}} \quad q = 2 + 0 = 2$$

5 Write down the final integral

$$- (-1)^q \frac{i}{\hbar} \lim_{\eta \rightarrow 0} \prod_{i=1}^n \int d\omega_i f_{\alpha_i}^{p_i}(\omega_i) \prod_{j=0}^{2n-2} \frac{1}{A_j + i\eta} \quad (4.63)$$

$$2^{\text{nd}} \text{ order} \Rightarrow -\frac{i}{\hbar} \lim_{\eta \rightarrow 0} \int d\omega \frac{f_{\alpha}^{-}(\omega)}{-\omega + E_2 - \bar{E}_2 + i\eta}$$

$$4^{\text{th}} \text{ order} \Rightarrow -\frac{i}{\hbar} \lim_{\eta \rightarrow 0} \int d\omega \int d\omega' \frac{1}{-\omega + \omega' + i\eta} \frac{f_{\alpha}^{+}(\omega)}{-\omega + E_2 - \bar{E}_2 + i\eta} \frac{f_{\alpha'}^{-}(\omega')}{\omega' - E_2 + \bar{E}_2 + i\eta}$$

[6] The tunnelling matrix elements associated to a vertex,  $T_{\alpha s}^{\mp}(b, a)$  has a superscript  $\mp = \pm$  depending on the creation/annihilation character of the vertex. The subscript  $\alpha s$  indicate the lead and the spin quantum number of the electron in the tunnelling event. The arguments  $a$  and  $b$  represent the state - with respect of the contour alignment - before and after the vertex respectively.